The Numerical Simulation of NonCharring Thermal Degradation and its Application to the Prediction of Compartment Fire Development

F. Jia, E. R. Galea and M. K. Patel
Fire Safety Engineering Group, Centre for the Numerical Modelling and Process Analysis
University of Greenwich, London SE18 6PF. U.K.
http://fseg.gre.ac.uk

ABSTRACT

In this paper we present some work concerned with the development and testing of a simple solid fuel combustion model incorporated within a Computational Fluid Dynamics (CFD) framework. The model is intended for use in engineering applications of fire field modelling and represents an extension of this technique to situations involving the combustion of solid fuels. The CFD model is coupled with a simple thermal pyrolysis model for combustible solid noncharring fuels, a six-flux radiation model and an eddy-dissipation model for gaseous combustion. The model is then used to simulate a series of small-scale room fire experiments in which the target solid fuel is polymethylmethacrylate. The numerical predictions produced by this coupled model are found to be in very good agreement with experimental data. Furthermore, numerical predictions of the relationship between the air entrained into the fire compartment and the ventilation factor produce a characteristic linear correlation with constant of proportionality 0.38 $kg/sm^{5/2}$. The simulation results also suggest that the model is capable of predicting the onset of "flashover" type behaviour within the fire compartment.

KEYWORDS: CFD, field model, pyrolysis, solid fuel combustion, flashover, post-flashover

1. INTRODUCTION

Solid fuel combustion is of central importance to fire research. By its very nature, this involves physical and chemical processes in both the solid and gaseous phases. For a specified room fire scenario, it is desirable to predict the fire development in terms of measurable material properties, the geometric configuration of the compartment and the physical state of the environment. In an earlier paper [1,2], the authors presented an attempt to simulate – in two-dimensions using the field modelling methodology - the thermal degradation processes of solid fuels such as wood, and to couple the gas-phase and solid-phase behaviours to simulate fire development within compartments. The model was shown to

be capable of qualitatively predicting the flame spread process and produce behaviours similar to flashover and backdraft. In this paper the work is continued and the model is extended to three-dimensions and model predictions are compared with experimental data [3] for compartment fires involving polymethylmethacrylate (PMMA).

Simulation of fire growth and spread within enclosures is a very difficult task. Not only are the gas-phase and solid-phase combustion processes complex in their own right, but in addition we must also contend with the interaction between turbulence, gas-phase combustion, radiation and solid phase behaviours. Over the past 15 years considerable effort has been expended in developing computational fluid dynamics (CFD) based fire field models capable of predicting the development of hazardous conditions within fire enclosures [4-8]. The majority of practical fire modelling applications have been concerned with the spread of heat and smoke in complex structures and so combustion has either been ignored or greatly simplified. In cases where combustion is ignored the fire is treated as a simple prescribed source of heat and smoke. While this approximation may appear crude it can produce good agreement with experimentally derived temperature measurements [9,10] for room fire scenarios. Generally, when combustion is included, it is approximated using relatively simple one-step reaction mechanisms [8,11] for liquid or gaseous fuels such as methane.

While these simple combustion models increase the complexity of the simulation, they still ignore or greatly simplify many important combustion aspects. One of the major simplifications is the use of fluid rather than solid fuels. In these cases, in addition to the simplifications associated with turbulence, chemical mechanisms, reaction rate, soot formation and thermal radiation, the charring and pyrolysis processes, as well as flame spread over solid surfaces are ignored.

A number of models have been proposed to treat the complex chemical and physical changes in pyrolyzing solid fuels [12,13]. A simple one-step global model of the pyrolyzing mechanism is widely used. The evolution of the non-charring material thermal degradation is described by the reaction, solid fuel goes to volatiles. Under the assumption of the one-step global mechanism, there are numerous models based on the partial differential equations for conservation of mass, momentum and energy. In general, these models can be classified into two regimes: kinetic and ablative. The kinetic models try to incorporate the kinetic mechanisms of the thermal degradation of solid fuels. By ignoring the complex chemical reactions in the pyrolyzing material, the ablation models are simpler than the kinetic models. The assumption in the ablation models is that noncharring solid fuels are gasified only at the surface region. Furthermore, combustible gaseous products are released only when the solid surface is heated to the critical pyrolysis temperature (ignition temperature) and the temperature of the pyrolyzing regions remains at the pyrolysis temperature throughout the mass loss stage. In addition, the chemical changes within the pyrolyzing regions are not taken into account. The solid fuel is considered to be chemically inert. The mass transfer in the barrier layer (melted film) over virgin material is ignored. Only heat transfer within the condensed phase is treated.

The mathematical expressions for the thermal degradation rate in ablative models are very similar. The mass loss rate is determined by the energy balance at the solid surface or at the boundary of char and virgin material. However, ablative models differ in their assumptions and solution methods. The integral model developed by Delichatsios et al. [14] for

noncharring materials uses exponential temperature profiles across the sample thickness for the heating-up stage and the pyrolysis stage. The use of these specified temperature profiles transforms the governing partial differential equations for the solid fuel into ordinary differential equations with variables θ (surface temperature rise), δ (thermal length) and δ_p (the depth of the material pyrolyzed). Similar integral methods using quadratic rather than exponential temperature profiles within the solid have been employed to derive integral models by Quintiere [15], Quintiere and Iqbal [16] and Moghtaderi *et al.* [17]. Another approach [1,18] involves solving the heat conduction equation in the condensed phase and the boundary conditions using the finite difference method. The temperature profiles in the solid are not prescribed. The mass loss at each node depends on the energy balance at that point.

While some recent work has attempted to predict fire spread in enclosures through the use of zone and field models [19-21], these have incorporated the rate of flame spread over the solid fuel through the use of thermal analysis, empirical formulations or direct use of Cone Calorimeter data. A different approach [1,2,18] has been developed where the flame spread is governed by a set of partial differential equations which describe and link gas-phase and solid-phase behaviour. This approach is followed in this paper. However, where the earlier work of Jia et al [1,2] was confined to two-dimensional examples, this work is extended to three-dimensional analysis and the numerical predictions compared with experimental data.

2. MODEL DESCRIPTION

The models presented here have been incorporated within the CFX [22] software (Version 2.3.3). This is a general purpose CFD package which solves the set of three-dimensional, partial differential equations that govern fluid flow. Compressibility is assumed and the perfect gas law is used to describe the equation of state. In this software, all solid surfaces are modelled with non-slip conditions for the velocities. The usual 'wall functions' are used to compute shear stresses at solid surfaces. The entire model consists of the following sub-components, a gas-phase combustion model, a radiation model and a thermal pyrolysis model. Detailed model description can be found in ref. 1 and 2. Here a brief outline of the model is presented. The gas phase combustion is modelled by the eddy dissipation concept [23]. Radiative heat transfer is calculated using the six-flux model modified with temperature-dependent medium absorption coefficient. The mass loss of PMMA is simulated with a noncharring pyrolysis model belonging to the ablative family. The model is further described in section 3.2.

3. SIMULATION OF FIRE GROWTH IN A SMALL COMPARTMENT

Quintiere et al.[3] conducted a series of fire growth tests within a small compartment using PMMA as the solid fuel. In this section, numerical models described above are used to reproduce the experimental results from a selection of the test series.

3.1 The Experiments

Square slabs of PMMA were burned in a small compartment constructed of low density

alumina silica block. The internal dimensions of the enclosure were 0.30m×0.30m×0.56m deep with a doorway height of 0.225m and widths ranging from 0.015 m to 0.285m (see figure 1). PMMA samples of various sizes were burned, ranging in face area from 0.0025m^2 to 0.0225m^2 with a constant thickness of 0.013m. The PMMA was burned on a platform 0.03m above the floor and centered 0.40m from the doorway. The weight was continuously recorded by a load cell that supported the platform. Two bare chromel-alumel thermocouples were used to measure the upper gas and ceiling temperatures (see figure 1). The ceiling thermocouple was pressed flush into the surface. A water-cooled heat flux sensor was used to record the incident heat flux to the floor. Pressure differences across the compartment wall were measured using an electronic manometer.

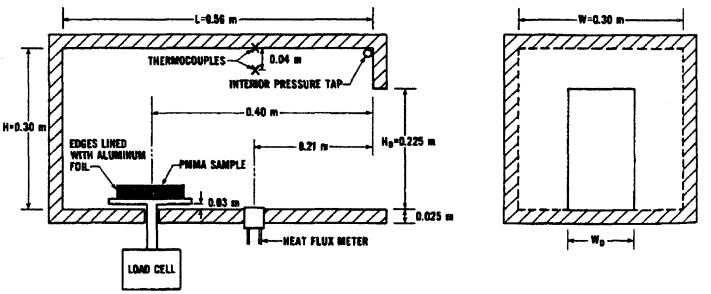

Figure 1: The experimental arrangement (from ref. 3).

3.2 The Simulations

The burning of the PMMA square samples is simulated with the noncharring pyrolysis model described in section 2. The material properties used in the simulations take the values provided by Quintiere et al. [3]. They are: ρ = 1192.0 kg/m^3, c= 1460.0 J/(kgK), λ = 0.19 W/(mK), T_p = 636.0 K, L = 1008.0kJ/kg.

The radiative heat transfer is modelled by the six-flux radiation model. The calculation of the absorption coefficient (k, units m^{-1}) of the hot air in the upper layer (k_g) follows the suggestion of Quintiere et al. [3], that is,

$$k_g = 0.30+4.64\,\dot{m}_b\,(\dot{m}_a+0.6\,\dot{m}_b). \tag{1}$$

where $\dot{m}_a$ is the rate of the entrained air flow and $\dot{m}_b$ is the burning rate of the combustible gases within the compartment. The soot absorption coefficient (k_s) is evaluated using the expression proposed by Yuen and Tien [24],

$$k_s = cT \tag{2}$$

where c is a constant and T is the gas-soot mixture temperature. The value of the constant c is determined using the flame absorption coefficient a (1.3 m^{-1}) and the flame temperature T_m

(1400K) provided by Quintiere et al. [3]. Thus the soot absorption coefficient is expressed as,

$$k_s = aT/T_m \tag{2a}$$

The total absorption coefficient of the soot-gas mixture is given by,

$$k = k_s + k_g. \tag{3}$$

The convective heat transfer coefficient of the walls and ceiling is calculated using [3],

$$h_w = 1.44(\dot{m}_b \Delta H)^{1/3} \ . \tag{4}$$

The floor convective heat transfer coefficient assumes the value 10, as suggested by Quintiere et al. The walls, ceiling and floor are treated as conductive regions with properties given by $\rho_w = 260 kg/m^3$, $k_w = 0.14 W/mK$. The thickness of the wall, ceiling and floor is 0.025m.

At the end of each iteration, the convective heat flux can be expressed as,

$$\dot{q}_c'' = h_w(T_s - T_g) \tag{5}$$

where T_g is the gas main stream temperature near the solid surface and h_w is the convective heat transfer coefficient calculated according to equation (4) or assigned a constant value for the floor. The solid surface temperature T_s can be obtained from the pyrolysis model if the solid is combustible or from the integral model [25] if the solid is non-combustible. The convective heat flux calculated in terms of equation (5) is then used to set up the boundary condition of heat transfer at the solid surface for the flow domain. This procedure is placed into the iterative process of the CFX software in each iteration.

The smaller PMMA samples combined with the narrower door openings produce laminar-like flame plumes. However, the gas-phase combustion model is based on the turbulent dissipation concept. Thus, only the two larger sample sizes of $0.0225m^2$ and $0.0156m^2$, and four larger door openings of 0.285m, 0.185m, 0.115m and 0.077m, are selected for simulation. As a result, a total of seven tests were simulated. The computational meshes for the flow domain used in these simulations vary with the individual test. The maximum number of cells used in these simulations consisted of 17×16×32 while the minimum number of cells consisted of 15×16×30.

The discretisation of the PMMA sample is dependent on the size of the sample. The surface of the PMMA sample was discretised using either 5x5 cells (small sample) or 7x5 cells (larger sample). In each case, a cell thickness of 0.2mm was used as recommended by the sensitivity analyses for solid grids, resulting in 65 cells through the thickness of the sample. The platform where the PMMA samples were placed is treated as a nonconducting region. As no information concerning the surface area of the platform was available, the platform is assumed to have the same surface area as the sample in each individual test. The actual height of the platform is 0.03m. Since surface regression of the samples is neglected, the platform height is assumed to be 0.043m which is the sum of the actual platform height and the thickness of the sample.

3.3 Simulation Results

The numerical predictions and corresponding experimental results are presented in table 1. The experimental values presented in table 1 refer to average values of the variable concerned, as measured during the period of maximum steady burning. In addition to these maximum values, their deviation during this period is also listed. The corresponding numerical predictions listed in table 1 are determined in a similar way. In table 1, the experimentally derived rate of entrained air flow was calculated by Quintiere et al. using other measurements such as upper layer gas temperature, PMMA mass loss rate and the pressure rise across the compartment wall. The numerical predictions for the entrained air rate presented in table 1 are determined by summing the mass flow rates into the compartment throughout the open doorway.

TABLE 1: Comparison of numerical predictions with experimental results.

Test No.		31A	14A	30A	23A	29A	22A	27A
Door Width (m)		0.077		0.115		0.185		0.285
Fuel Area (m^2)		0.0156	0.0225	0.0156	0.0225	0.0156	0.0225	0.0225
$\dot{m}_v$ g/s	pred.	0.69	0.759	0.848	1.1	1.0	1.39	1.69
	exp.	0.79	0.875	1.0	1.225	0.908	1.5	1.56
T_g °C	pred.	853	869	990	906	1136	1056	1050
	exp.	910±50	902±50	993±25	902±50	973±25	950±75	1022±25
T_w °C	pred	750	823	906	823	813	807	820
	exp.	865±50	854±35	937±25	854±50	863±25	902±50	$925\pm^{25}_{50}$
$\dot{q}''_F$ W/cm^2	pred.	6.7	9.04	11.55	9.07	8.49	8.40	9.09
	exp.	9.88±.65	8.05±1.2*	11.0±0.8	9.62±.78	$8.45\pm^{1.0}_{2.6}$	10.8±.78	10.4±1.3
Δp N/cm^2	pred.	1.56	1.57	1.65	1.64	1.71	1.79	1.69
	exp.	[0.72±.2]	1.8±.12	[1.0±.2]	2.24±.08	[1.16±.08]	1.88±.08	1.92±.12
$\dot{m}_a$ g/s	pred.	3.45	3.46	5.18	5.0	7.89	7.42	11.01
	exp.	--	2.53	--	7.26	--	7.29	11.9
HRR (pred.) kW	inside	9.62	9.56	13.89	13.69	18.97	20.08	25.96
	outside	4.96	6.09	5.13	7.68	4.46	8.99	10.35

Note: $\dot{m}_v$ is the average mass loss rate in the period of maximum steady burning; T_g is the gas temperature in the upper layer temperature; T_w is the ceiling temperature; $\dot{q}''_F$ is the incident heat flux at the floor; Δp is the pressure rise across the compartment wall; $\dot{m}_a$ is the rate of the entrained air flow and HRR is the heat release rate of the gas-phase combustion. [ ]:pressure tap clogged; *: water coolant hose melted.

4. DISCUSSION

As can be seen from Table 1, the agreement between the predicted and corresponding measured values are good. Large differences occur for the pressure rises of test 29A, 23A, 30A and 31A. However, except for test 23A, the measured pressure rises are not reliable due to pressure taps being clogged. For the other three tests (14A, 22A and 27A), the predicted pressure rises are close to the measured ones. The predicted air inflow rate for test 14A and

23A are quite different from the measured values while as demonstrated later they are consistent with other empirical correlation.

Given the range of the experimental results, the general trends predicted by the numerical model appear to follow those produced in the experimental results. These trends concern the change in T_g and $\dot{q}''_F$ as the door width is kept constant but the fuel size is increased and conversely when the fuel size is kept constant and the door width is increased. For the tests with doorway width of 0.115m (i.e. tests 30A and 23A) and 0.185m (i.e. 29A and 22A), the predicted upper layer gas temperature and the heat flux at the floor for fuel surface area of $0.0156m^2$ (i.e. tests 30A and 29A) are generally greater than the values for fuel face area of $0.0225m^2$ (i.e. 23A and 22A). At first sight this may be contrary to expectation as the larger fuel sample would be expected to produce the higher temperatures and heat fluxes.

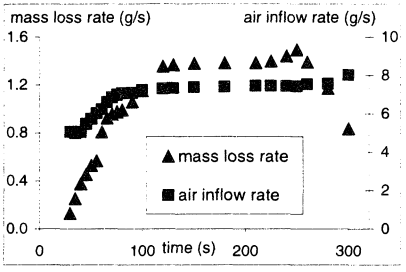

Figure 2: Predicted mass loss rate vs. time for the test conditions with 0.185m doorway width and $0.0225m^2$ PMMA sample (i.e. test 22A).

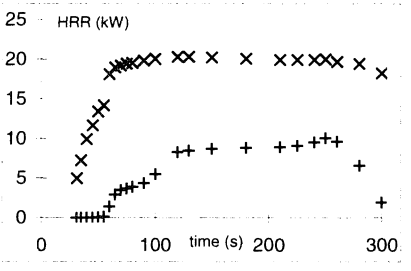

Figure 3: Predicted heat release rate within (symbol: x) and outside (symbol: +) the compartment for test conditions with 0.185m doorway and $0.0225m^2$ PMMA sample (i.e. test 22A).

The transient history of the mass loss rate and heat release rate within and outside the compartment for test 22A is depicted in figures 2 and 3. Only the results for test 22A are presented as the results for the other test cases are similar in nature. Note the rapid increase in the heat release rate within the compartment (see figure 3) and the corresponding rapid increase in the mass loss rate (figure 2). However, as the heat release rate reaches a maximum, quasi-steady value, the mass loss rate continues to increase steadily. As this is occurring, the rate of air flow entrained into the compartment also remains nearly constant (see figure 2).

These occurrences suggest that the fire is ventilation controlled. As described by Quintiere et al, "...so much fuel is vaporized that it can not be burned within the compartment due to insufficient oxygen. This excess fuel serves to dilute the products of combustion and hence to reduce the temperature and rate of heat flux received by the fuel surface from the compartment."[3]. For the same doorway width, the larger fuel sample produces more combustible volatiles. Consequently, the effect of dilution due to unburned vaporised fuel is also greater and causes a lower upper layer gas temperature and heat flux at the floor. The

numerical predictions also show that slightly more fresh cool air is entrained into the compartment ($\dot{m}_a$) for the tests using smaller samples, which also helps to reduce the upper layer temperature.

However, for the tests with 0.077m doorway width (i.e. tests 31A and 14A), the cooling effect due to unburned pyrolysis products within the compartment is not great enough as the mass loss rates are not sufficiently large. As a result, the test using the larger sample (i.e. test 14A) creates higher upper layer temperatures and heat flux at the floor than the test with the smaller sample size (i.e. test 31A). The numerical simulations for these two tests also reproduced this feature.

Another interesting observation from figures 2 and 3 concerns the onset and development of "flashover" type conditions. Within a very short time period, the mass loss rate and the heat release rate within the compartment undergo rapid increases. The end of this short growth period approximately corresponds to when the flux of entrained fresh air into the compartment reaches a steady state. At this stage the amount of entrained fresh air limits the burning rate and the combustion within the compartment becomes ventilation controlled. While this is occurring, the mass loss rate continues to increase steadily. As a result the predicted heat release rate within the compartment remains nearly constant while the predicted heat release rate outside the compartment continues to increase (see figure 3) suggesting flames emerging from the compartment. All these observations are consistent with the flashover phenomena. In their analyses, Quintiere et al.[3] also suggested that flashover occur in this test.

After the heat release rate within the compartment reaches a steady state, the mass loss rate from the solid fuel continues to increase until it attains a quasi-steady state (see figures 2 and 3). At this point, the heat release rate outside the compartment also maintains a quasi-steady state (see figure 3). This is to be expected as the total heat release rate of the gas-phase combustion is controlled by the generation rate of the combustible vapour that is approximately constant during this period. Eventually, the heat release rate of the internal fire begins to diminish as the fuel is exhausted note however, that the external combustion is exhausted before the internal combustion. The computer generated fire development described above corresponds to the classic description of compartment fire development. After ignition, an initial growth period is followed by a rapid transition (or flashover) into the fully developed fire. The fully developed fire is characterised by a steady burning fire within the compartment with flames emerging from within the compartment. Such fires are often ventilation controlled. Finally, as the combustible fuel is exhausted, the fire enters the decay phase. These observations are consistent to those produced by the earlier two-dimensional model [1,2].

According to Babrauskas [26] and Thomas [27], the energy release rate required for flashover in a compartment is estimated by,

$$Q = 750 A_o \sqrt{H_o} , \tag{6}$$

or

$$Q = 0.78 A_T + 378 A_o \sqrt{H_o} \tag{7}$$

where A_T is the total internal surface area of the compartment, A_o is the area of the vent and H_o is the height of the vent.

These equations suggest that for a small scale compartment, such as the one used in these experiments (0.56m×0.3m×0.3m), conditions suitable for the development of flashover may easily develop due to the low heat release rate required. For the test compartment with 0.185m door width, equations 6 and 7 suggest that the heat release rate necessary for flashover is 14.8kW and 14.1kW respectively. It should be noted that while it may not be appropriate to use equation 6 in this application due to the small scale of the test compartment, it may provide a rough estimation as to condition required for flashover. These values are consistent with the low level of heat release rate (approximately 12kW) predicted at the onset of flashover - assuming that flashover occurs during the short transition from fuel controlled to ventilation controlled fire (see figure 3).

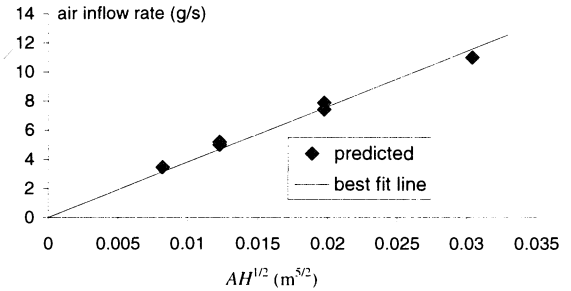

Figure 4: The rate of air flow entrained into the compartment vs. the ventilation factor.

Using data generated from the numerical predictions, it is possible to suggest a relationship between the predicted entrainment rates and the ventilation factor $A_oH_o^{1/2}$ for the compartment. The predicted rates of entrained air flow versus the ventilation factor $A_oH_o^{1/2}$, where A_o is the area of the door opening and H_o is the height of the door are plotted in figure 4. The air inflow rates are determined during the period of maximum steady burning and hence are in the post-flashover phase of fire development. The figure strongly suggests a proportional relationship for post-flashover fires between the rate of entrained air flow and the ventilation factor. The same trend for post-flashover fires was shown by Rockett [28]. He calculated the constant of proportionality to be in the range 0.4 to 0.61 kg/sm$^{5/2}$ depending on the selected discharge coefficient for the opening. Using the line of best fit in figure 4, we determine the constant of proportionality to be 0.38 kg/sm$^{5/2}$. This value is close to the lower limit obtained by Rockett. Therefore, the air inflow rate at the post-flashover stage can be approximately expressed as,

$$\dot{m}_a = 0.38 A_o H_o^{1/2} \qquad (8)$$

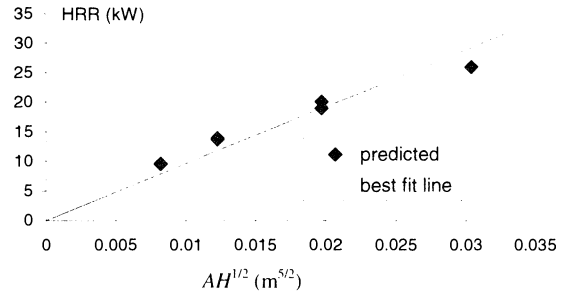

Figure 5: The heat release rate of gas-phase combustion within the compartment predicted by the gas-phase combustion model versus the ventilation factor.

By assuming that the air entrained into the compartment has a constant oxygen concentration, it is possible to suggest a relationship between the heat release rate due to the gas-phase combustion and the ventilation factor. The rate of the air entrainment into the compartment determines the total combustion rate within the compartment. If the air entrained into the compartment has a constant oxygen concentration, the heat of combustion per unit mass of air consumed will be approximately constant. Thus, at steady-state, the heat release rate due to combustion within the compartment is expected to have a linear relationship with the ventilation factor. Depicted in figure 5 is a plot of the predicted heat release rate due to gas-phase combustion versus the ventilation factor. It shows that a nearly linear relationship exists between the predicted heat release rate and the ventilation factor.

Finally, table 1 demonstrates that the predicted heat release rates within the compartment are very similar for those tests with different size samples but with the same doorway width. This is to be expected as the predicted air inflow rates for tests with the same door width are very similar. As the rate of entrained air establishes an upper limit on the burning rate within the compartment, similar rates of the air inflow result in similar heat release rates within the compartment. However, the predicted heat release rates outside the compartment increase with increases in sample size for a given doorway width. This is because the tests with larger samples release more combustible gases than the tests with the smaller samples. While more gases are released, as discussed above only a certain amount of gas can be consumed within the compartment. Consequently, the excess combustible gases are vented out of the compartment where they burn on contact with the abundant ambient oxygen, resulting in a greater heat release rate outside for the tests with larger samples.

5. CONCLUSIONS

A pyrolysis model for noncharring solid fuels has been developed and shown to produce very good agreement with measured mass loss rates for PMMA samples. In order to simulate the complex processes of fire growth within a compartment, the pyrolysis model was coupled with a gas-phase combustion model and a thermal radiation model within a three-dimensional CFD environment. Radiative heat transfer is the central and dominant mode of heat transfer

in compartment fires and was modelled by the relatively simple six-flux model. The numerical predictions produced by the model were compared with a range of experimental results of fire growth within a small compartment. The fire scenarios consisted of various sized PMMA fuel loads with several different door sizes. The model predictions were found to be in very good agreement with the experimental results. Furthermore, a linear correlation - similar to that determined by Rockett - was found between the predicted entrained air rate and the ventilation factor. Finally, the model was shown to possess the ability to predict flashover type behaviour within the compartment.

While the pyrolysis model adopted here appears to provide a promising approach to the prediction of fire growth of the first item burning within enclosures, much work remains before it can be applied to engineering applications of fire field modelling. The model's reliance on simple treatments of radiation and gaseous combustion must be further assessed through for example the inclusion of; a discrete transfer radiation model, ignition and extinction mechanisms for gaseous combustion. The model must also be further developed to include physical behaviour such as charring and downward flame spread and its suitability for other fuels must be established. Furthermore, additional quantitative validation of the model with experimental data must be performed. Work along all these lines is currently under way.

6. ACKNOWLEDGEMENTS

Mr Jia gratefully acknowledges the financial support of the University of Greenwich through its research bursary system. Professor E Galea is indebted to the UK CAA for their financial support of his chair in mathematical modelling at the University of Greenwich.

7. REFERENCES

1. Jia, F., Galea, E.R. and Patel, M.K., "The prediction of fire propagation in enclosure fires", Fire Safety Science-Proc. of the Fifth International Sym. pp. 439-450, 1997.
2. Jia, F., Galea, E. R. and Patel, M K., "The numerical simulations of enclosure fires using a CFD fire field model coupled with a pyrolysis based solid fuel combustion submodel – a first approximation", Journal of Fire Protection Engineering, vol. 9, no. 4., 1999.
3. Quintiere, J. G., McCaffrey B. J. and Braven, K. D., "Experimental and theoretical analysis of quasi-steady small-scale enclosure fires", 17th Sym. (Int.) on Comb, pp. 1125-1137, 1979.
4. Galea, E.R., "On the field modelling approach to the simulation of enclosure fires", J. Fire Protection Engng, vol. 1, pp. 11-22, 1989.
5. Galea, E.R. and Markatos, N.C., "The mathematical modelling and computer simulation of fire development in aircraft", Int.J.Heat Mass Transfer, vol. 34, pp.181-197, 1991.
6. Markatos, N.C. and Cox, G., "Hydrodynamics and heat transfer in enclosures", Physico-Chem. Hydrody. Vol. 5, pp. 53-66, 1984.
7. Simcox, S, Wilkes, N,S and Jones, I.P., "Computer simulation of the flows of hot gases from the fire at King's Cross Underground Station", Fire Safety J., vol. 18, pp. 49-73, 1992.
8. Yeoh, G. H., Chandrasekaran, V. and Leonardi, E., "Numerical prediction of fire and smoke", AIRAH Journal, vol. 49, pp.13-18, 1995.

9. Kerrison, L., Mawhinney, N., Galea, E.R., Hoffmann, N. and Patel, M.K., "A comparison of two fire field models with experimental room fire data", Fire Safety Science--Proc 4th Int Symp, pp. 161-172, 1994.
10. Kerrison, L., Galea, E. R., Hoffmann, N. and Patel, M. K., "A comparison of a FLOW3D based fire field model with experimental room fire data", Fire Safety J., vol. 23, pp. 387-411, 1994.
11. Kumar, S., Gupta, A.K. and Cox, G., "Effects of Thermal Radiation on the Fluid Dynamics of Compartment Fires", Fire Safety Science- Proc 3rd Int Symp, pp. 345-354, 1991.
12. Blasi, C. D., "Modelling and simulation of combustion processes of charring and noncharring solid fuels", Prog. Energy Combust. Sci., vol. 19, pp 71-104, 1993.
13. Kashiwagi, T., "Polymer combustion and flammability-role of the condensed phase", 19th symposium (international) on combustion, The Combustion Institute, p. 1423, 1994.
14. Delichatsios, M.M., Mathews, M.K. and Delichatsios, M.A., "An upward fire spread and growth simulation", Fire Safety Science-Proc. of the Third Inter Sym. pp. 207-216, 1991.
15. Quintiere, J. G. "A semi-quantitative model for the burning of solid materials", NIST-4840, National Institute of Standards and Technology, June, 1992.
16. Quintiere, J. G. and Iqbal, N."An approximate integral model for the burning rate of a thermoplastic-like material", Fire and Material, vol. 18, pp. 89-98, 1993.
17. Moghtaderi, B., Novozhilov, V., Fletcher, D. and Kent, J. H., "An integral model for the transient pyrolysis of solid materials", Fire and Materials, vol. 21, p.7, 1997.
18. Yan, Z. and Holmstedt, G., "CFD and experimental studies of room fire growth on wall lining materials", Fire Safety J., vol. 27, pp. 201-238, 1996.
19. Karlsson, B., "Modeling fire growth on combustible lining materials in enclosures", 992, Report TVBB-1009, Lund University, Dept of Fire Safety Engg, Lund, Sweden, 1992.
20. Luo, M. and Beck, V., "Flashover fires in a full scale building: prediction and experiment", Proceedings Interflam'96, Compiled by C.Franks and S Grayson, ISBN 0 9516320 9 4, 1996, pp. 361-370.
21. Opstad, K., "Modelling of thermal flame spread on solid surfaces in large-scale fires", MTF-Report 1995:114(D), Department of Applied Mechanics, Thermo- and Fluid Dynamics, The Norwegian Institute of Technology, University of Trondheim, 1995.
22. Burns, A.D and Wilkes, N.S, "A finite-difference method for the computation of fluid flows in complex three dimensional geometries", U.K. Atomic Energy Authority Harwell Report. AERE-R 12342, 1987.
23. Magnussen, B. F. and Hjertager, B. H., "On mathematical modelling of turbulent combustion with special emphasis on soot formation and combustion", 16th Symp. (Int.) on Combustion, the Combustion Institute, pp. 719-729, 1977.
24. Yuen, W. W. and Tien, C. L., "A simple calculation scheme for the luminous flame emissivity", 16th Sym. (Int.) on Combustion, pp1481-1487, 1977.
25. Özişik, M. N., Heat conduction, John Wiley & Sons, Inc., 1980, New York.
26. Babrauskas, V., "Estimateing room flashover potential", Fire Technology, vol. 16, pp. 94-104, 1980.
27. Thomas, P.H., "Testing products and materials for their contribution to flashover in room", Fire and Materials, vol. 5, pp. 103-111, 1981.
28. Rockett, J. A., "Fire induced gas flow in an enclosure", Combustion Science and Technology, vol. 12, pp. 165-175, 1976.